Thermally Excited Modes in a Pure Electron Plasma

F. Anderegg, N. Shiga, J. R. Danielson, D. H. E. Dubin, and C. F. Driscoll
Institute for Pure and Applied Physical Sciences and University of California at San Diego, La Jolla, California 92093

R. W. Gould
California Institute of Technology, Mail Stop 128-95, Pasadena, California 91103
(Received 3 December 2001; published 17 March 2003)

Thermally excited plasma modes are observed in near-thermal-equilibrium pure electron plasmas over a temperature range of $0.05 < kT < 5$ eV. The measured thermal emission spectra together with a plasma-antenna coupling calibration uniquely determine the temperature. This calibration is obtained from the spectra themselves when absorption of the receiver-generated noise is significant, or from kinetic theory. This nondestructive temperature diagnostic agrees well with standard diagnostics and may be useful for expensive species such as antimatter.

DOI: 10.1103/PhysRevLett.90.115001 PACS numbers: 52.25.Gj, 52.25.Kn, 52.27.Jt, 52.35.Fp

Unneutralized plasmas are unique in that they can be trapped in a rotating near-thermal-equilibrium state by static electric and magnetic fields. Steady-state confinement of $N = 10^3$–10^9 electrons, ions, or antimatter particles [1,2] is routinely used in plasma experiments, atomic physics [3], and spectroscopy [4]. The thermal equilibrium characteristics become most evident with the formation of Coulomb crystals [5] when pure ion plasmas are cooled to the liquid and solid regimes at sub-Kelvin temperatures, but the higher temperature plasma regime studied here is also well described by near-equilibrium statistical mechanics [6].

These stable near-thermal-equilibrium plasmas exhibit fluctuating electric fields which are excited and damped by the random motions of the particles. Weakly damped plasma waves are the normal modes of the system; in traps with finite length and radius, these appear as discrete Trivelpiece-Gould (TG) standing mode frequencies [7]. In an isolated equilibrium plasma, the modes would have an average electrostatic potential energy of $\frac{1}{2}kT$ per mode; here, the mode coupling to the receiver electronics can be comparable to the coupling to the (rotating) thermal equilibrium plasma.

Somewhat simpler center-of-mass "trap modes" are commonly observed in the single-particle regime with highly tuned resonant circuits in hyperbolic traps [8], diagnosing the number of particles, but not their temperature. At higher frequencies, thermal excitation of cyclotron modes is readily observed in warm non-neutral [9] and hot fusion plasmas [10]. In space plasmas, thermal noise diagnostics [11] are substantially different because of the lack of boundaries.

In this Letter, the spectrum of thermally excited TG standing modes is measured in pure electron plasmas over a temperature range of $0.05 < kT_p < 5$ eV, using a room-temperature receiver. The received spectrum for each mode is nominally a Lorentzian at frequency ω_m with width γ_m, superimposed on the receiver-generated noise modified by plasma absorption.

By Nyquist's theorem, the thermal noise driving a mode is proportional to kT_p and proportional to the real part of the mode/antenna impedance Z_m [9]. The impedance Z_m can be obtained directly from the received spectra when the receiver impedance and noise are significant, or it can be calculated from a kinetic theory of random test particles incorporating the plasma dielectric. Overall, the technique allows a rapid nondestructive diagnostic of the plasma temperature with $\pm 25\%$ accuracy; with a low temperature amplifier, it would be applicable to diagnosing the positrons down to Kelvin temperatures in traps to create antihydrogen [2].

Thermal emission spectra were obtained from pure electron plasmas contained in two similar Penning-Malmberg traps, "*IV*" and "*EV*," differing mainly in plasma diameter and magnetic field strength. The *IV* trap consists of a series of hollow conducting cylinders of radius $r_w = 2.86$ cm contained in ultrahigh vacuum at $P \approx 10^{-10}$ torr with a uniform axial magnetic field of $B = 30$ kG [Fig. 1(a)]. Electrons are injected from a hot tungsten filament and contained axially by voltages $V_c \approx -200$ V on end electrodes. Typical plasmas have $N \approx 10^9$ electrons in a column length $L_p \approx 41$ cm, with a plasma radius $r_p \approx 0.2$ cm and a central density $n_0 \approx 10^7$ cm^{-3}. (For *EV*, typical parameters are $B = 0.375$ kG, $r_p = 1.7$ cm, $r_w = 3.8$ cm, and $L_p = 24$ cm.)

The plasma density profile $n(r)$ and the temperature T_p are obtained by dumping the plasma axially and measuring the charge and energy of the escaping particles [12]. The *EV* plasmas expand radially towards the wall with a characteristic "mobility" time of $\tau_m \approx 100$ sec, so the electrons are repetitively injected, diagnosed, and dumped. On *IV*, a weak "rotating wall" (RW) drive at $f_{\mathrm{RW}} \sim 0.5$ MHz provides steady-state confinement of the electron column [13]. To control the temperature, we apply auxiliary "wiggle" heating by modulating one containment voltage V_c at a frequency $f_h = 0.8$–1.0 MHz.

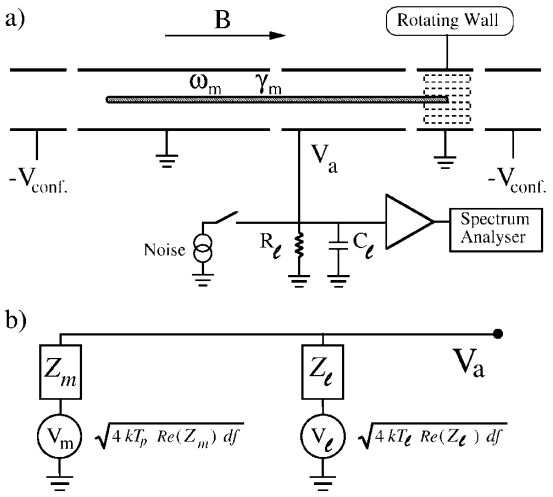

FIG. 1. Schematic diagram of the cylindrical Penning-Malmberg trap with (a) the wave reception electronics and (b) the thermal emission equivalent circuit.

The azimuthally symmetric $m_\theta = 0$ standing plasma wave resonances used here are readily identified with a standard transmission experiment, with rf excitation and reception on separate wall cylinders. Figure 2(a) shows the spectrum with wall excitation of $V_{\rm exc} = -80$ dBm (22 μV) at frequencies $f = 0.01$–10 MHz. The Trivelpiece-Gould mode frequencies can be approximated as [7]

$$\omega_m \approx \omega_p\left(\frac{r_p}{r_w}\right)(r_w k_z)\left[\frac{1}{2}\ln\left(\frac{r_w}{r_p}\right)\right]^{1/2}\left[1+\frac{3}{2}\left(\frac{\bar{v}}{v_\phi}\right)^2\right], \quad (1)$$

scaling with density as the plasma frequency $\omega_p \equiv 2\pi \cdot 28$ MHz $(n/10^7\ {\rm cm}^{-3})^{1/2}$, reduced by the fractional fill ratio r_p/r_w and by the wall shielding ratio $r_w k_z$. Resonant standing modes occur only at discrete axial wave numbers $k_z = \pi m_z/L_{\rm eff}$, with finite-length corrections $L_{\rm eff} \approx L_p + O(R_w)$ [14] and m_z an integer. Here, we consider only the lowest radial mode number $m_r = 1$, since higher m_r couple only weakly to wall antennas. Thermal frequency shifts and Landau damping depend on the ratio of $v_\phi/\bar{v}$, where $v_\phi \equiv \omega_m/k_z$ and $\bar{v} \equiv (kT_p/m)^{1/2}$.

The modes are nominally linear, with density perturbations of $\delta n/n \lesssim 10^{-4}$ driven by $V_{\rm exc} \leq -80$ dBm. However, Landau damping of the mode is generally nonlinear even down to near-thermal levels, due to wave-particle trapping near velocity v_ϕ [15]. The apparent lesser sensitivity for $m_z = 2$ is due to the location and length ($L_a = 11.7$ cm) of the cylindrical detection antenna. The peak labeled RW is the rotating wall drive; similar spectra are obtained with the drive off.

Small peaks representing thermally excited modes are still visible in Fig. 2(b) when the transmitter electrode is grounded ($V_{\rm exc} = 0$). These peaks have amplitudes of -124 dBm with a bandwidth BW = 3 kHz, representing voltage fluctuations on the electrode with spectral intensity $V_a/\sqrt{df} \approx 2.6\ {\rm nV}/\sqrt{\rm Hz}$.

Figure 3 shows received spectra of the thermally excited $m_z = 1$ mode for four different plasma temperatures. The mode frequency ω_m increases slightly with temperature, as expected from Eq. (1). The width of the spectral peak represents mode damping, and this width increases substantially as Landau damping becomes significant for $kT_p \gtrsim 0.5$ eV, i.e., for $v_\phi/\bar{v} \lesssim 5$. At high temperatures, the spectrum is broad, but weak; roughly speaking, the "area" $\int df V_a^2$, corrected for the load impedance, will be proportional to kT_p.

Figure 1(b) shows a circuit modeling the reception of thermal noise from the plasma. The thermal fluctuation voltage V_m flows through a mode/antenna impedance $Z_m(\omega)$, and through a receiver load impedance $Z_\ell(\omega)$ with its inevitable noise V_ℓ. Near a mode at frequency ω_m with intrinsic damping γ_m, the mode admittance Z_m^{-1} is given by a simple pole, as

$$Z_m^{-1}(\omega) = \frac{\mathcal{G}\omega_m^2}{i(\omega-\omega_m)+\gamma_m}. \quad (2)$$

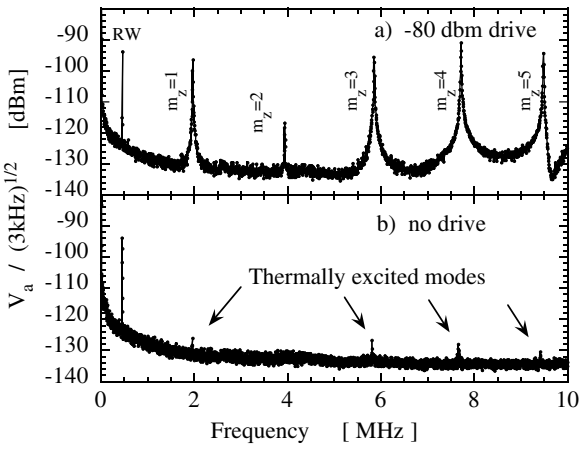

FIG. 2. (a) Spectrum of $m_\theta = 0$, $m_z = 1, 2, \ldots, 5$ Trivelpiece-Gould modes. (a) driven; (b) no drive.

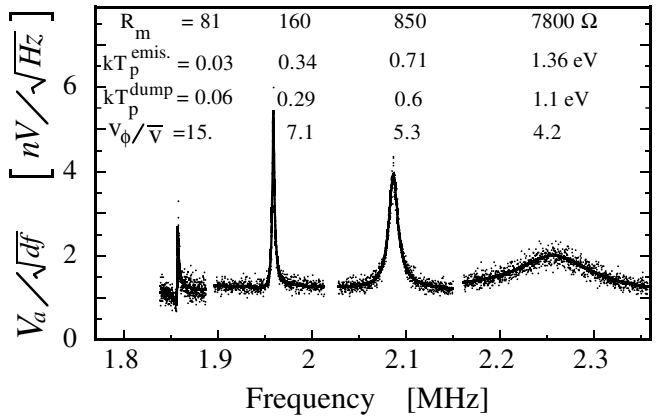

FIG. 3. Spectra of the thermally excited $m_\theta = 0$, $m_z = 1$, mode for different plasma temperatures; the solid lines are fits to Eq. (6).

The geometric coupling between the plasma mode and the receiving electrode is represented by the capacitance $\mathcal{G} \approx 0.4$ pF. The mode impedance on resonance is purely real, with magnitude

$$R_m \equiv Z_m^{\mathrm{Re}}(\omega_m) = \frac{\gamma_m}{\mathcal{G}\omega_m^2}, \tag{3}$$

where $Z^{\mathrm{Re}} \equiv \mathrm{Re}\{Z\}$ and $Z^{\mathrm{Im}} \equiv \mathrm{Im}\{Z\}$. The known load resistance R_ℓ and capacitance C_ℓ give a load impedance

$$Z_\ell \equiv (R_\ell^{-1} + i\omega C_\ell)^{-1}, \tag{4}$$

which is essentially constant over the mode resonance; for *IV*, 750 Ω/440 pF gives $Z_\ell(\omega_m) \approx (40 - 170i)\ \Omega$.

Nyquist's theorem says that the spectral density of the square of the noise voltage is proportional to kT times the real part of the impedance, for both the mode and the load noise sources. A voltage-divider fraction $|Z_\ell/(Z_m + Z_\ell)|$ of the mode voltage V_m will be measured on the antenna as V_a together with an analogous fraction of the (uncorrelated) load noise, giving

$$\frac{V_a^2(f)}{df} = 4kT_p Z_m^{\mathrm{Re}} \left| \frac{Z_\ell}{Z_m + Z_\ell} \right|^2 + 4kT_\ell Z_\ell^{\mathrm{Re}} \left| \frac{Z_m}{Z_m + Z_\ell} \right|^2. \tag{5}$$

Using Eqs. (2) and (4), Eq. (5) can be explicitly written as

$$\frac{V_a^2(f)}{df} = 4kT_p R_m \frac{|Z_\ell|^2}{|R_m + Z_\ell^{\mathrm{Re}}|^2} \frac{\gamma_{\mathrm{tot}}^2}{\gamma_{\mathrm{tot}}^2 + (\omega - \omega_m')^2} + 4kT_\ell Z_\ell^{\mathrm{Re}} \left\{ 1 - \frac{2(\omega - \omega_m')\delta\omega_m + (\gamma_{\mathrm{tot}}^2 - \gamma_m^2 - \delta\omega_m^2)}{\gamma_{\mathrm{tot}}^2 + (\omega - \omega_m')^2} \right\}, \tag{6}$$

where

$$\begin{aligned} \gamma_{\mathrm{tot}} &\equiv \gamma_m + \gamma_\ell \equiv (1 + Z_\ell^{\mathrm{Re}}/R_m)\gamma_m, \\ \delta\omega_m &\equiv \omega_m - \omega_m' \equiv Z_\ell^{\mathrm{Im}} \omega_m^2 \mathcal{G}. \end{aligned} \tag{7}$$

The first term of Eq. (6) describes the Lorentzian plasma emission spectrum centered at ω_m' of width γ_{tot}, with amplitude proportional to $kT_p R_m$. Thus, this emission spectrum alone does not determine kT_p unless prior knowledge of the coupling coefficient $\mathcal{G}$ allows R_m to be obtained from Eq. (3). The second term describes a uniform noise background, plus a "dip and peak" from the $(\omega - \omega_m')$ term, plus a Lorentzian absorption, with all three components proportional to $kT_\ell Z_\ell^{\mathrm{Re}}$. The differing spectral shapes of the two terms allow noise generated by T_p to be distinguished from that generated by T_ℓ. Indeed, this load noise spectrum determines T_ℓ (since Z_ℓ^{Re} is known) *and* it determines $\mathcal{G}$ if this spectral shape is discernible; for this reason, adding noise at the receiver can improve this determination of $\mathcal{G}$.

Figure 4 shows measured emission spectra from the *EV* apparatus with (upper, heavy lines) and without (lower, light lines) added receiver "noise"; both are accurately described by Eq. (6) (solid lines). The quiet receiver gives a low background, determining $kT_\ell = 0.15$ eV, but the frequency variation of the second term of Eq. (6) (short dashes) is smaller than the data scatter, so $\mathcal{G}$ is not accurately determined. The upper spectrum resulted from injecting white noise current at the receiver electrode, with spectral density around ω_m corresponding to a resistor Z_ℓ^{Re} at $kT_\ell = 6.9$ eV. Fitting Eq. (6) to the data then gives essentially the same Lorentzian plasma emission (shifted left by 5 kHz due to shot-to-shot plasma variations), and the second term of Eq. (6) (upper short dashes) determines $\mathcal{G} = 0.40$ pF accurately. The load noise is reduced ("shorted") by the mode impedance on the left-hand side of the Lorentzian peak.

Thus, the plasma temperature T_p is uniquely determined by the received spectrum alone for regimes where the load-generated noise "filtered" by the plasma resonance is significant compared to the plasma emission; this was the case only for the $kT_p = 0.03$ eV data of Fig. 3. In practice, the most effective technique is to add noise with $T_\ell \approx T_p$, so that ω_m, γ_m, T_p, T_ℓ, and $\mathcal{G}$ are all determined directly from each set of spectral data. This technique essentially combines a reflection/absorption measurement to determine $\mathcal{G}$ with the plasma emission measurement.

Alternately, one can calculate the coupling coefficient $\mathcal{G}$ analytically using kinetic theory. Analysis of a uniform density collisionless plasma of radius r_p with z-periodic boundaries of period L_p reproduces the impedance of Eq. (2) for frequencies near a plasma resonance. In the limit of $T \to 0$, assuming that $\lambda_d \ll r_p$ and that $k_z r_w \ll 1$, we find that

$$\mathcal{G} = \frac{4\pi\varepsilon_0 L_p F_m^2}{1 + x^2 \ln^2(r_\omega/r_p)}, \tag{8}$$

where $F_m \equiv (m_z\pi)^{-1}[\sin(m_z\pi z_2/L) - \sin(m_z\pi z_1/L)]$

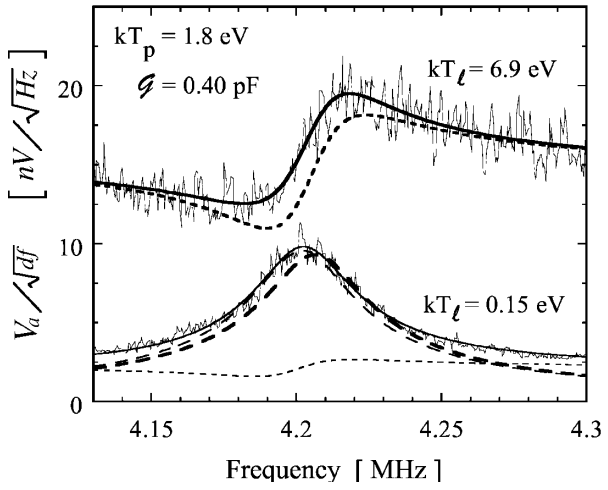

FIG. 4. Spectra of the thermally excited mode for $kT_p = 1.8$ eV (bottom); and with noise added to the receiver (top).

with z_1 and z_2 the left and right ends of the antenna cylinder. Here, x is a dimensionless quantity that satisfies the equation $xJ_1(x)\ln(r_w/r_p) = J_0(x)$ and is related to the frequency of the plasma mode by $x = k_z r_p(\omega_p^2/\omega_m^2 - 1)^{1/2}$. For $r_\omega/r_p \gg 1$, $x \approx \sqrt{2/\ln(r_w/r_p)}$, which implies $\mathcal{G} \simeq L_p F_m^2/[1 + 2\ln(r_w/r_p)]$. For a typical EV plasma, this gives $\mathcal{G} = 0.42$ pF, whereas we measure $0.40 \leq \mathcal{G} \leq 0.73$ as the plasma temperature varies over $3.5 \geq kT_p \geq 0.7$ eV.

A more complete kinetic analysis of a Maxwellian distribution of "fully dressed" test particles including the plasma dielectric properties [16] reproduces the Nyquist theorem of Eq. (5) and also gives the fluctuation spectrum off resonance. For example, the $m_z = 1$ spatial Fourier component has total (frequency-integrated) charge fluctuations $(\delta N)^2 = (\delta q)^2/e^2 \sim \mathcal{O}(0.1)(\lambda_D/r_p)^3 N$ for $\lambda_D \lesssim r_p$, showing a strong reduction below the $(\delta N)^2 \propto N$ fluctuations expected for fully uncorrelated particles [17].

Figure 5 displays the inferred plasma temperatures T_p^{emis} obtained from emission spectra and reflection/absorption measurements, versus the plasma temperatures T_p^{dump} measured by dumping the plasma. Data were taken for plasmas with several "geometric" parameters (n, r_p, L_p) on EV (circles) and IV (triangles), with varied amounts of plasma heating. Most of the values of T_p^{emis} were obtained from four-parameter fits to the emission spectra, together with a separate absorption/reflection determination of $\mathcal{G}$; measurements with a noisy load combine both measurements, and a single five-parameter fit gives the same results.

It is important to note that the load resistance Z_ℓ^{Re} contributes to the observed mode damping γ_{tot} on an equal footing with the internal (Landau) damping represented by R_m, as shown in Eq. (7). Thus, the external dissipation from $Z_\ell^{\text{Re}} = 40\ \Omega$ induces a baseline mode damping of $\gamma_\ell/\omega_m = 6 \times 10^{-4}$.

In the two-coupling model of Eq. (5), the plasma mode is coupled to the thermal plasma [6] at rate γ_m, and to the load resistor at rate γ_ℓ, so the time-averaged mode energy W_m evolves as $\dot{W}_m = \gamma_m(kT_p - W_m) + \gamma_\ell(kT_\ell - W_m)$, with equilibrium value

$$W_m = (\gamma_m kT_p + \gamma_\ell kT_\ell)/(\gamma_m + \gamma_\ell). \tag{9}$$

Other couplings could easily modify the mode energy ($\sim kT$) without significantly affecting the overall plasma thermal energy ($\sim 10^9$ kT). Thus, steady-state plasmas can exhibit spectral peaks which are 10 to 100 times larger than thermal, when external signals stimulate particular plasma modes without proportionately heating the plasma [as in Fig. 2(a)]. Similarly, particular modes in a warm plasma have been damped (i.e., cooled) by up to 25× with an external feedback circuit, without substantially cooling the plasma. Thus, the accuracy of the temperature diagnostic may be limited by unwanted rf couplings to the plasma mode.

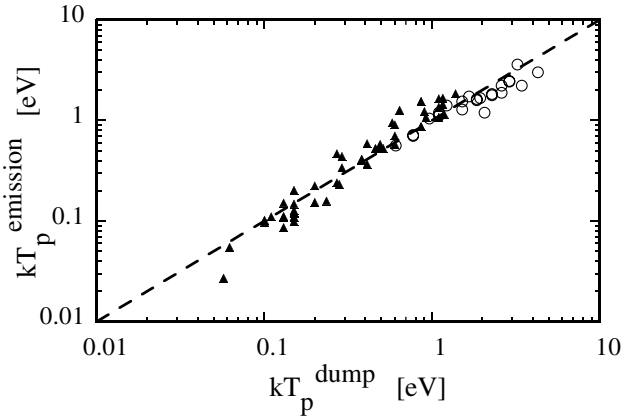

FIG. 5. Plasma temperature measured by emission/reflection technique, compared to the standard dump temperature measurement. The triangles are from the IV apparatus and the circles are from the EV apparatus.

This work is supported by ONR Grant No. N00014-96-1-0239 and NSF Grant No. PHY-9876999. We thank R. E. Pollock and T. M. O'Neil for many fruitful discussions.

[1] R. G. Greaves and C. M. Surko, Phys. Plasmas **4**, 1528 (1997).
[2] M. Amoretti *et al.*, Nature (London) **419**, 456 (2002); G. Gabrielse *et al.*, Phys. Rev. Lett. **89**, 213401 (2002).
[3] J. P. Sullivan, S. J. Gilbert, and C. M. Surko, Phys. Rev. Lett. **86**, 1494 (2001).
[4] K. H. Knoll *et al.*, Phys. Rev. A **54**, 1199 (1996).
[5] T. B. Mitchell *et al.*, Science **282**, 1290 (1998).
[6] T. M. O'Neil and D. H. E. Dubin, Phys. Plasmas **5**, 2163 (1998).
[7] S. A. Prasad and T. M. O'Neil, Phys. Fluids **26**, 665 (1983); A.W. Trivelpiece and R.W. Gould, J. Appl. Phys. **30**, 1784 (1959).
[8] D. J. Wineland and H. G. Dehmelt, J. Appl. Phys. **46**, 919 (1975).
[9] R.W. Gould, Phys. Plasmas **2**, 2151 (1995).
[10] I. Fidone, G. Giruzzi, and G. Taylor, Phys. Plasmas **3**, 2331 (1996).
[11] N. Meyer-Vernet and C. Perche, J. Geophys. Res. **94**, 2405 (1989).
[12] A.W. Hyatt, C. F. Driscoll, and J. H. Malmberg, Phys. Rev. Lett. **59**, 2975 (1987).
[13] F. Anderegg, E. M. Hollmann, and C. F. Driscoll, Phys. Rev. Lett. **81**, 4875 (1998).
[14] J. K. Jennings, R. L. Spencer, and K. C. Hansen, Phys. Plasmas **2**, 2630 (1995).
[15] J. R. Danielson, Ph.D. thesis, University of California at San Diego, 2002.
[16] N. Krall and A.W. Trivelpiece, *Principles of Plasma Physics* (McGraw-Hill, New York, 1973), Chap. 11.
[17] N. T. Nakata, G.W. Hart, and B. G. Peterson, in *Non-Neutral Plasma Physics IV*, edited by F. Anderegg, L. Schweikhard, and C. F. Driscoll, AIP Conf. Proc. No. 606 (AIP, Melville, NY, 2002), p. 271.